Output Feedback Control for Main Spool Displacement of Two Stage Hydraulic Valves Driven by Proportional Pilot Valves*

Xinhao Ji, Haibo Xie, Chengzhen Wang, and Yuexing Wang

Abstract— **The performance of a dual-stage hydraulic valve depends on the displacement tracking precision of the main spool. Due to limited internal space, the dual-stage hydraulic valve is usually only equipped with the displacement sensor. However, in traditional electro-hydraulic control system models, the pressure signal is a state variable that usually needs to be measured directly. In addition, traditional models also have mismatched uncertainties, which hinder the application of observer-based modern control methods in the main spool displacement control system. In this article, the chain-integral model was established for the main spool displacement control system to avoid issues with pressure measurement and mismatched uncertainties. Then, an extended-state-observer based back-stepping control method was developed for the chain integral model, and Lyapunov-based stability analysis was given. Finally, a test platform was set up and comparative experiments were executed to validate the availability of the developed controller. The comparative experimental results display that the developed approach can enhance tracking accuracy.**

I. Introduction

The hydraulic valve is the core component for flow and pressure control in hydraulic systems [1-4]. In two-stage hydraulic valves, the main stage spool is typically driven by the electro hydraulic proportional pilot stage [5-6]. The performance of the dual-stage hydraulic valve mainly depends on the control accuracy of main stage spool displacement [7]. Thus, in the industrial application of two-stage hydraulic valves, there is an urgent need for the high performance main spool displacement controller [8].

To achieve better control performance of the main spool displacement control (MSDC) system, scholars and engineers have made active attempts and achieved some beneficial results. In [9], a control method based on segmented proportional-integral-derivative (PID) is designed to enhance the step response characteristics of the MSDC system. In [10], the PID parameters of the MSDC system were optimized through multiple orthogonal experiments, which can obtain the optimal PID parameters without prior knowledge and modeling of the MSDC system. In [11], the fuzzy PID controller with integral-separation is proposed to enhance the dynamic and static performance of two-stage hydraulic valves. In [12-13], the PID control method with dead zone detection and compensation was developed to handle the control dead zone issue of two-stage hydraulic valves, which effectively reducing the adverse effects of dead zone on main spool position control.

In traditional hydraulic system models, the pressure signal is a state variable and is usually required to be directly measurable. However, due to limited internal space, the dual-stage electro-hydraulic valve is usually only equipped with the displacement sensor. Therefore, the pressure signals in the two end chambers of the main spool cannot be obtained in real time. Moreover, traditional models also have mismatched uncertainties. These adverse factors hinder the application of advanced modern control techniques based on state-space models, such as observer-based controller [14-15], sliding mode controller [16-17], adaptive robust controller [18-19], and so on. This is also the reason why most two-stage hydraulic valves adopt PID or PID-based feedforward control methods to achieve closed-loop control of the MSDC system. But, due to the inability to achieve full state feedback and uncertainty compensation, it is difficult for PID controllers to fulfill the requirements of high-precision spool displacement tracking. With the intention of applying modern control techniques based on state-space models to enhance the tracking precision of the MSDC system, some researchers have tried to obtain state variables by performing derivative operations on the spool displacement [20]. However, the derivative calculation of the displacement signal can also amplify the sensor noise, which may undermine control system stability.

To solve the above problems, this paper develops an output feedback control method based on the chain integral model. The contributions of this paper are reflected in the following three aspects. First, a chained integration model was established for the MSDC system to avoid problems with pressure measurement and mismatched uncertainties. Thus, the ESO can be directly employed to estimate state variables and lumped uncertainties. Secondly, based on the estimated value from ESO, a back-stepping controller is designed, which can achieve full-state feedback and uncertainty compensation. Furthermore, based on Lyapunov theory, the stability analysis of the designed controller is provided. Finally, comparative experiments were executed on the experimental platform to test the tracking behavior of the developed control method.

*This work was supported by the National Key R&D Program of China under Grant 2023YFB3406602.

Xinhao Ji is with the State Key Laboratory of Fluid Power and Mechatronic Systems, Zhejiang University, Hangzhou 310027 China (e-mail: jixinhao@zju.edu.cn)

Haibo Xie is with the State Key Laboratory of Fluid Power and Mechatronic Systems, Zhejiang University, Hangzhou 310027 China, also with the Zhejiang Key Laboratory of Intelligent Manufacturing Industrial Software, Hangzhou 311199 China, and also with the Institute of Advanced Machine Zhejiang University, Hangzhou 311199 China (phone: 86-571-87952274; fax: 86-571-87951941; e-mail: hbxie@zju.edu.cn)

Chengzhen Wang is with the Institute of Advanced Machine Zhejiang University, Hangzhou 311199 China (e-mail: czwang@zju.edu.cn)

Yuexing Wang is with the State Key Laboratory of Fluid Power and Mechatronic Systems, Zhejiang University, Hangzhou 310027 China (e-mail: 12225126@zju.edu.cn)

II. Dynamic Modeling and Problem Statement

A. System Modeling

The principle of the MSDC system is depicted in Fig. 1, in which the main stage spool is driven by an electro-hydraulic proportional pilot stage. The mechanical dynamics of the main spool is described as

$$m\ddot{x}_p = P_L A - kx_p - F_h - F_f \tag{1}$$

where x_p and m denote the displacement and inertial mass of the main-stage spool, $P_L = P_1 - P_2$ indicates the pressure difference between the two end chambers of the main spool, P_1 and P_2 denote the pressure of the right and left end chambers, respectively, A indicates the equivalent area of the two end chambers of the main stage spool, k represents the stiffness of the return spring, F_h and F_f are flow force and friction, respectively.

When the MSDC system is operating normally, the leakage of the right and left end chambers of the main spool is very small. Therefore, neglecting the leakage of the two end chambers, the flow equation is

$$\begin{cases} Q_1 = A\dot{x}_p + \dfrac{V_{10} + Ax_p}{\beta_e}\dot{P}_1 \\ Q_2 = A\dot{x}_p - \dfrac{V_{20} - Ax_p}{\beta_e}\dot{P}_2 \end{cases} \tag{2}$$

where Q_1 denotes the flow entering the left chamber, Q_2 indicates the flow exiting from the right chamber, β_e indicates the bulk modulus of oil and V_{10} and V_{20} represent the volumes of the two end chambers when the main spool is in the initial position, in the MSDC system $V_{10} = V_{20}$.

The working pressure of the two end chambers is

$$\begin{cases} P_1 = \dfrac{P_p + P_L}{2} \\ P_2 = \dfrac{P_p - P_L}{2} \end{cases} \tag{3}$$

where P_p is the pressure of the pilot oil source.

Define $Q_L = (Q_1 + Q_2)/2$, combining (2) and (3), we have

$$Q_L = A\dot{x}_p + \frac{V_t}{4\beta_e}\dot{P}_L \tag{4}$$

where $V_t = V_{10} + V_{20}$ represents the overall volume of the left and right end chambers.

Define function $\mathrm{sgn}(*)$ as

$$\mathrm{sgn}(*) = \begin{cases} 1 & * > 0 \\ 0 & * = 0 \\ -1 & * < 0 \end{cases} \tag{5}$$

Then, the flow of the proportional pilot stage is modeled as

$$Q_L = C_d \omega x_v \sqrt{\left(P_p - \mathrm{sgn}(x_v)P_L\right)/\rho} \tag{6}$$

where C_d denotes the flow coefficient, x_v indicates the spool displacement of the pilot stage, ω represents the flow area gradient of the proportional pilot valve, ρ indicates the density of oil.

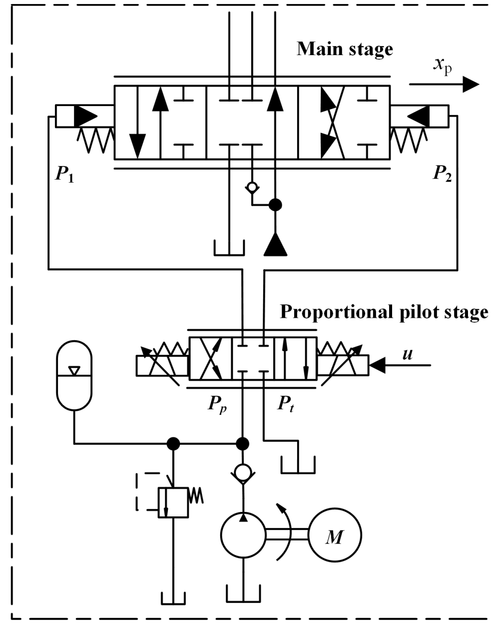

Figure 1. Hydraulic principle of the MSDC system

Considering that the response speed of the proportional pilot stage is much higher than that of the main stage spool. Thus, the dynamics of the proportional pilot stage are approximated as

$$x_v = k_{xv}u \tag{7}$$

where u denotes the input current of the pilot valve, k_{xv} indicates the conversion coefficient between input current and spool displacement.

Select the displacement, velocity, and acceleration of the main stage spool as system state variables, such as $\boldsymbol{x}^{\mathrm{T}} = [x_1, x_2, x_3] = [x_p, \dot{x}_p, \ddot{x}_p]$. Then, the chain integral model of the MSDC system is modeled as

$$\left.\begin{aligned} \dot{x}_1 &= x_2 \\ \dot{x}_2 &= x_3 \\ \dot{x}_3 &= \frac{1}{m}\left[-\theta_1 x_2 + \theta_2 g(P_L, x_v)k_{xv}u - \dot{F}\right] \end{aligned}\right\} \tag{8}$$

where $\theta_1 = 4A^2\beta_e/V_t + k$, $g(P_L, x_v) = \sqrt{P_p - \mathrm{sgn}(x_v)P_L}$, $\theta_2 = 4A\beta_e C_d\omega/\left(V_t\sqrt{\rho}\right)$, $F = F_h + F_f$.

Remark 1. Generally, displacement, velocity, and load pressure are selected as system states to establish the system model of the hydraulic system. However, due to limited internal space, the dual-stage hydraulic valve is usually only equipped with the displacement sensor. Therefore, the pressure signals in the two end chambers of the main spool cannot be obtained in real time. In addition, traditional models also have mismatched uncertainties, which hinder the application of observer-based modern control methods. Therefore, in this paper, a chain integration model as shown in (8) is established to avoid issues with pressure measurement and mismatched uncertainties.

B. Model Problems Statement

There are two main obstacles to accomplishing the task of high-performance tracking of the system (8). One is that some system states cannot be directly measured, such as speed x_2 and acceleration x_3. Another is that there are uncertainties in the system (8), such as θ_1, θ_2, $g(P_L, x_v)$, and F. Although speed and acceleration can be obtained by taking the derivative of the spool output displacement, the differentiation operation also amplifies the noise of the displacement sensor. The uncertainty and noise can impair the tracking behavior and stability of the MSDC system.

To tackle these challenges, an output feedback controller based on the extended-state-observer (ESO) was designed to achieve high-performance tracking of the MSDC system. With a view to facilitate the subsequent design of the control algorithm, all uncertainties in (8) are consolidated into a total uncertainty $d(t)$. Thus, the system (8) is rewritten as

$$\left.\begin{aligned} \dot{x}_1 &= x_2 \\ \dot{x}_2 &= x_3 \\ \dot{x}_3 &= \hat{b}u + d(t) \end{aligned}\right\} \tag{9}$$

Where $\hat{b}$ indicates the estimated value of b, $b = \theta_2 g(P_L, x_v)k_{xv}/m$, $\tilde{b} = \hat{b} - b$ represents the error between b and $\hat{b}$, $d(t) = -\left(\theta_1 x_2 + \dot{F}\right)/m - \tilde{b}u$ denotes the total uncertainty.

The subsequent work of this article is to design a suitable output feedback controller that effectively handles the uncertainty $d(t)$ in system (9) to enable the output displacement x_1 to track the instruction displacement x_d as precisely as possible.

III. Controller Design

Within this section, the design process of the developed control algorithm is given, which mainly includes an ESO and an output feedback control algorithm. Before proceeding with the controller design, a realistic assumption is given as

Assumption 1. $d(t)$ is a piecewise differentiable function with a finite number of discontinuous points.

Remark 1. During normal operation of the system, all state variables and system parameters in model (8) are continuous and bounded, and the hydraulic forces and friction forces acting on the main spool can be described as a piecewise function. Therefore, considering $m \neq 0$, it is reasonable to *Assumption* 1.

A. Extended State Observer

To solve the problem that the state variables and uncertainties in system (9) cannot be directly measured, a fourth-order ESO was applied to estimate uncertainties and state variables in real-time. Define $x_4 = d(t)$, the (9) can be extended as

$$\left.\begin{aligned} \dot{x}_1 &= x_2 \\ \dot{x}_2 &= x_3 \\ \dot{x}_3 &= \hat{b}u + x_4 \\ \dot{x}_4 &= h(t) \end{aligned}\right\} \tag{10}$$

where $h(t)$ indicates a bounded piecewise function.

Define $z_i (i = 1, \cdots 4)$ as the estimated value of $x_i (i = 1, \cdots 4)$. Then, a fourth-order ESO is developed for (10) as

$$\left.\begin{aligned} \dot{z}_1 &= z_2 - \lambda_1 \tilde{z}_1 \\ \dot{z}_2 &= z_3 - \lambda_2 \tilde{z}_1 \\ \dot{z}_3 &= z_4 + \hat{b}u - \lambda_3 \tilde{z}_1 \\ \dot{z}_4 &= -\lambda_4 \tilde{z}_1 \end{aligned}\right\} \tag{11}$$

where $\lambda_i (i = 1, \cdots, 4) > 0$ represent the gains of the observer, $\tilde{z}_1 = z_1 - x_1$ indicates the estimated error of displacement.

Combining (10) and (11), the dynamic of estimated errors is

$$\dot{\tilde{\boldsymbol{z}}} = \boldsymbol{A}\tilde{\boldsymbol{z}} - \boldsymbol{H} \tag{12}$$

where

$$\boldsymbol{A} = \begin{bmatrix} -\lambda_1 & 1 & 0 & 0 \\ -\lambda_2 & 0 & 1 & 0 \\ -\lambda_3 & 0 & 0 & 1 \\ -\lambda_4 & 0 & 0 & 0 \end{bmatrix}, \ \boldsymbol{H} = \begin{bmatrix} 0 \\ 0 \\ 0 \\ h(t) \end{bmatrix}$$

It can be easily checked that the (11) is controllable when $\lambda_i \neq 0$. Therefore, by using the pole placement method, appropriate λ_i can be selected to arrange the eigenvalues of the state matrix $\boldsymbol{A}$ in the left half-plane, thereby ensuring the stability of the designed ESO. Consequently, there exists a positive definite symmetric matrix $\boldsymbol{R}$ such that $\boldsymbol{RA} + \boldsymbol{A^T R} = -\boldsymbol{P}$, in whicn $\boldsymbol{P}$ represents an identity matrix.

Remark 2. In observer (11), all state variables can be obtained through integration operations. In other words, the ESO (11) obtains the differential value of output displacement through integration operation, thereby avoiding the problem of noise amplification from the displacement sensor. Moreover, according to (12), the observation error is governed by λ_i. In theory, by adjusting λ_i, it is possible to make the observation error arbitrarily small.

B. Output Feedback Control Laws

Based on the estimated values of the system state and uncertainty from the ESO (11), an output feedback control law was designed. Define the displacement control error e_1 as $e_1 = x_1 - x_d$. Then, we have

$$\dot{e}_1 = x_2 - \dot{x}_d \tag{13}$$

Select x_2 as a recursive control variable. Then, the desired spool speed x_{2d} is designed as

$$x_{2d} = -l_1 e_1 + \dot{x}_d \tag{14}$$

where l_1 indicates a controller parameter, which will be designed later.

Define the spool speed tracking error e_2 as $e_2 = x_2 - x_{2d}$. Then, the dynamic of spool speed error can be depicted as $\dot{e}_2 = x_3 - \dot{x}_{2d}$. Select x_3 as a recursive control variable. Then, the desired spool acceleration x_{3d} is designed as

$$x_{3d} = -l_2(z_2 - x_{2d}) + \dot{x}_{2d} - e_1 \tag{15}$$

where l_2 denotes a controller parameter, which will be designed later.

Define the spool acceleration tracking error e_3 as $e_3 = x_3 - x_{3d}$. Subsequently, the dynamic of spool acceleration

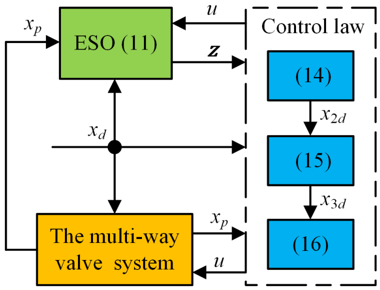

Figure 2. Controller flowchart

error can be depicted as $\dot{e}_3 = \hat{b}u + x_4 - \dot{x}_{3d}$. Therefore, the actual system input u is synthesized as

$$u = [-l_3(z_3 - x_{3d}) + \dot{x}_{3d} - (z_2 - x_{2d}) - z_4]/\hat{b} \quad (16)$$

where l_3 represents a controller parameter, which will be designed later.

In conclusion, the operational process of the designed control strategy is shown in Fig. 2.

C. Main Results

Define the constants $\lambda_{\min}$, σ , β , η and ξ as

$$\lambda_{\min} = \min\{\lambda_i(i=1,\cdots,4)\}, \sigma = 2\lambda_{\min}|\tilde{\boldsymbol{z}}^T\boldsymbol{PH}|_{\max}$$
$$\beta = \max\left\{\frac{l_2+1}{2}, \frac{l_3}{2}, \frac{1}{2}\right\}, \eta = \frac{(\lambda_{\min}-\beta)\tilde{\boldsymbol{z}}^T\tilde{\boldsymbol{z}}}{\lambda_{\min}\tilde{\boldsymbol{z}}^T\boldsymbol{P}\tilde{\boldsymbol{z}}}$$
$$\xi = 2\min\{l_1, l_2/2+1/2, l_3/2-1, \eta\} \quad (17)$$

If the controller parameters are tuned to satisfy $l_1 > 0$, $l_2 > 0$, $l_3 > 2$ and $\lambda_{\min} - \beta > 0$, the ESO (11) and control law (16) guarantees that:

(A): The estimated errors $\tilde{\boldsymbol{z}} = [\tilde{z}_1, \tilde{z}_2, \tilde{z}_3, \tilde{z}_4]$, and the control errors $\boldsymbol{e} = [e_1, e_2, e_3]$ are bounded. Specifically, the Lyapunov function $V(t) = (e_1^2 + e_2^2 + e_3^2)/2 + \lambda_{\min}\tilde{\boldsymbol{z}}^T\boldsymbol{P}\tilde{\boldsymbol{z}}$ is bounded by

$$V(t) \le V(0)\exp(-\xi t) + \frac{\sigma}{\xi}[1 - \exp(-\xi t)] \quad (18)$$

(B): When there is only the constant uncertainty in the system (9), such as $\dot{d}(t) = 0$, asymptotic convergence of estimation error and control error can be obtained, i.e. $\tilde{\boldsymbol{z}} \to \boldsymbol{0}$ and $\boldsymbol{e} \to \boldsymbol{0}$ as $t \to \infty$.

Proof: Combining (12), (16), and (17) we have

$$\begin{aligned}\dot{V} &= -l_1e_1^2 - l_2e_2^2 - l_3e_3^2 - \lambda_{\min}\tilde{\boldsymbol{z}}^T\tilde{\boldsymbol{z}} + 2\lambda_{\min}\tilde{\boldsymbol{z}}^T\boldsymbol{PH} \\ &\quad -l_2e_2\tilde{z}_2 - e_3\tilde{z}_2 - l_3e_3\tilde{z}_3 - e_3\tilde{z}_4 \\ &\le -l_1e_1^2 - l_2e_2^2/2 - (l_3/2-1)e_3^2 - \lambda_{\min}\tilde{\boldsymbol{z}}^T\tilde{\boldsymbol{z}} \\ &\quad -2\lambda_{\min}\tilde{\boldsymbol{z}}^T\boldsymbol{PH} + (l_2/2+1/2)\tilde{z}_2^2 + l_3\tilde{z}_3^2/2 + \tilde{z}_4^2/2 \\ &\le -l_1e_1^2 - l_2e_2^2/2 - (l_3/2-1)e_3^2 \\ &\quad -(\lambda_{\min}-\beta)\tilde{\boldsymbol{z}}^T\tilde{\boldsymbol{z}} - 2\lambda_{\min}\tilde{\boldsymbol{z}}^T\boldsymbol{PH} \end{aligned} \quad (19)$$

When the controller parameters satisfy $l_1 > 0$, $l_2 > 0$, $l_3 > 2$ and $\lambda_{\min} - \beta > 0$, combining (17) and (19), we have

$$\dot{V} \le -\xi V + \sigma \quad (20)$$

Because $\xi > 0$ and σ is bounded, the result *(A)* is proven.

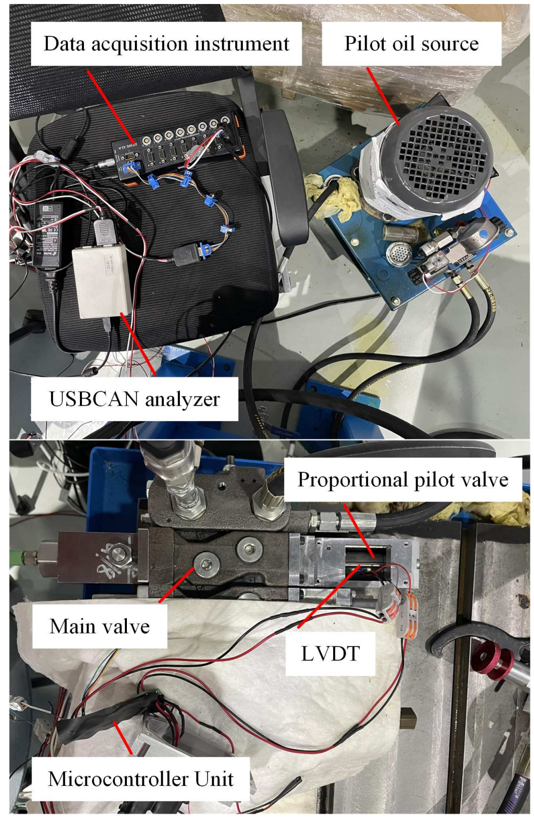

Figure 3. Test platform

If $\dot{d}(t) = 0$, then $\boldsymbol{H} = \boldsymbol{0}$ and $\sigma = 0$. According to (20), $V \to 0$ as $t \to \infty$. Therefore, result *(B)* is proven.

IV. Comparative Experiments

Within this section, a test platform was established for implementing comparative experiments. As given in the Fig. 3, the test platform is mainly composed of a main valve, a displacement sensor (LVDT), a proportional pilot valve, a pilot oil source, a micro-controller unit, a data acquisition instrument and a host. The pilot oil source is a constant pressure source, and the pressure is set to 30 *bar*. The control algorithm designed in the host is downloaded to the microcontroller unit through a USBCAN analyzer. The data acquisition instrument communicates with the host and sensors through a bus based on the CAN protocol, and the transmission cycle of CAN messages is set to 10 *ms*.

The instruction displacement trajectory of main spool given in the comparative experiment is $x_d = 2\sin(\pi t) + 3\,mm$. To demonstrate the effectiveness of the designed control algorithm, the most commonly used PID controller in industry was selected for comparison. And the following two experiments were implemented.

Exp. 1: The PID controller with parameters $k_p = 80$, $k_I = 50$, $k_d = 1$ was applied to track the x_d.

Exp. 2: The developed control algorithm is implemented. The gain of ESO are tuned as $\lambda_1 = 20$, $\lambda_2 = 150$, $\lambda_3 = 500$ and $\lambda_4 = 625$. The controller parameters are tuned as $l_1 = 10$, $l_2 = 40$ and $l_3 = 70$.

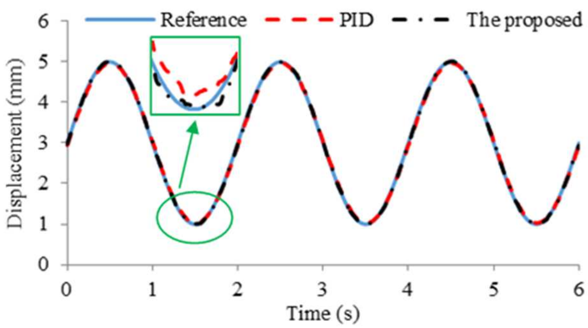

Figure 4. Comparison of displacement control performance

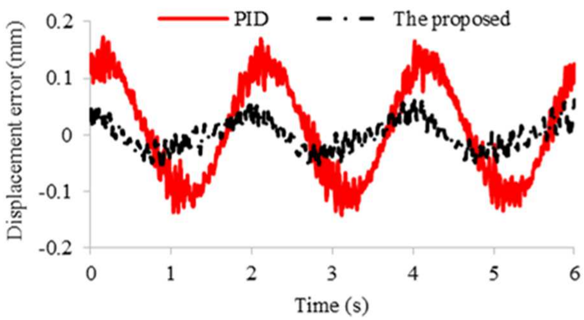

Figure 5. Comparison of displacement control errors

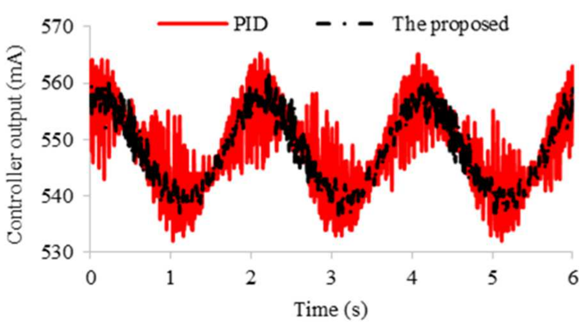

Figure 6. Controller output comparison

Remark 1. Before conducting the comparative experiment, the two controllers were well tuned through multiple experiments to ensure fairness in the comparison. The control parameters k_p, k_I and k_d in *Exp. 1*, as well as the control parameters l_1, l_2 and l_3 in *Exp. 2*, were all adjusted using the trial-and-error method. The ESO parameters $\lambda_i (i = 1, \cdots, 4)$ are determined by the pole placement method.

Furthermore, the following three error indices are defined to quantitatively analyze the tracking behavior of comparative experiments.

$$\left.\begin{aligned} I_{MAE} &= \max_{i=1,\ldots,n} \{|e_1(i)|\} \\ I_{MSE} &= \frac{1}{n}\sum_{i=1}^{N}[e_1(i)]^2 \\ I_{MSU} &= \frac{1}{n}\sum_{i=1}^{N}[u(i)]^2 \end{aligned}\right\} \tag{21}$$

where, I_{MAE} indicates the maximum displacement control error, I_{MSE} denotes the mean square value of the displacement control error, I_{MSU} represents the mean square value of the output signal of the controller, N indicates the number of data used for calculation.

Remark 2. In (21), the role of the index I_{MAE} is to assess transient response performance, while the index I_{MSE} is used to evaluate steady-state control performance. In addition, the control behavior of the controller is directly tied to its output strength. Therefore, the index I_{MSU} is utilized to assessthe output strength of the controller to ensure fairness in the controller comparison.

The control performance of *Exp.* 1 and *Exp.* 2 are depicted in Figs. 4 to 6. In *Exp.* 2, the estimation results of ESO on the state variable and uncertainty are exhibited in Fig. 7. The assess indices of tracking performance for *Exp.* 1 and *Exp.* 2 have been calculated and given in Table I. According to the results of the comparative tests, the indices I_{MAE} and I_{MSE} of

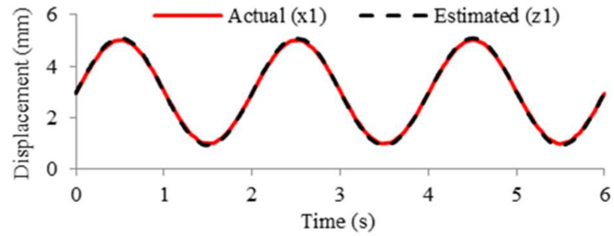

(a). The estimated result of x_1

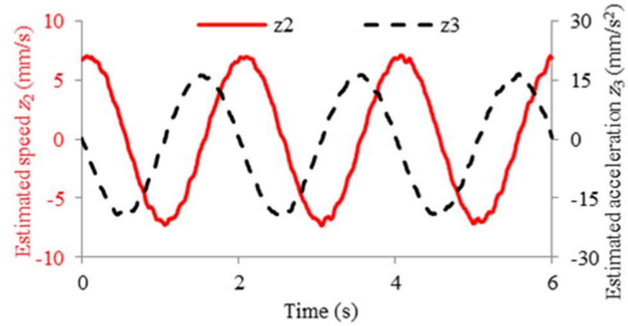

(b). The estimated result of x_2 and x_3

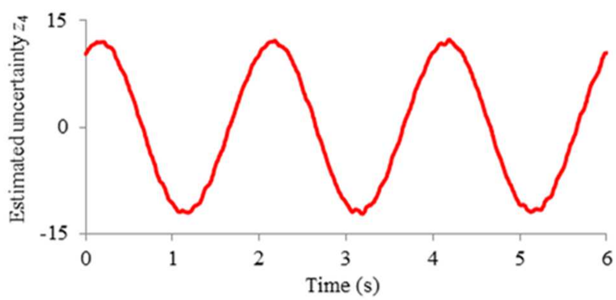

(c). The estimated result of uncertainty

Figure 7. The estimated results of ESO

TABLE I. TRACKING PERFORMANCE EVALUATION INDEX

Experiments	**Evaluation indexes**		
	$\boldsymbol{I_{MAE}}$	$\boldsymbol{I_{MSE}}$	$\boldsymbol{I_{MSU}}$
Exp. 1	0.17	7.47×10^{-3}	3.02×10^{5}
Exp. 2	0.06	6.93×10^{-4}	3.01×10^{5}

Exp. 2 are significantly smaller than those of *Exp.* 1 under almost the same control signal strength. Specifically, compared with *Exp. 1*, the *Exp. 2* reduced the maximum displacement control error by 60%. This confirms that the developed control method significantly enhances transient and steady-state performance compared to PID controllers. The main reason for the enhance of tracking behavior is that the designed control method can realize full state feedback and real-time uncertainty compensation based on the estimated values from ESO. It is noteworthy that, as depicted in Fig. 7, the estimation results of ESO are almost unaffected by sensor noise. This is because the ESO estimates the system state and uncertainty by integration operations, effectively avoiding the problem of noise amplification.

V. Conclusion

In this article, a chained integration model was established for the MSDC system to avoid problems with pressure measurement and mismatched uncertainties. Then, an ESO based back-stepping control strategy is designed for the chain integral model. The developed control method can achieve full-state feedback and uncertainty compensation with only the position feedback of main stage spool. The comparative test results display that compared with the commonly used PID control method, the developed controller reduces the maximum tracking error by 60% in the sinusoidal tracking process.

References

[1] R. Ding, G. Sun, J. Zhang, L. Peng, M. Cheng, B. Xu, and H. Yang, "A review of independent metering control system for mobile machinery," *Int. J. Hydromechatronics*, Vol. 8, No. 5, pp.1–39, 2025.

[2] Z. Quan, L. Ge, Z. Wei, Y. Li, and L. Quan, "A survey of powertrain technologies for energy-efficient heavy-duty machinery". *Proceedings of the IEEE*, Vol. 109, No. 3, pp.279–308, 2021.

[3] B. Xu, J. Shen, S. Liu, Q. Su, and J. Zhang, "Research and Development of Electro-hydraulic Control Valves Oriented to Industry 4.0: A Review," *Chin. J. Mech. Eng.*, Vol. 33, No. 29, 2020.

[4] J. Shi, L. Quan, X. Zhang, and X. Xiong. "Electro-hydraulic velocity and position control based on independent metering valve control in mobile construction equipment," *Automation in Construction*, Vol. 94, pp. 73-84, 2018.

[5] J. Zhang, Z. Lu, B. Xu, and Q. Su, "Investigation on the dynamic characteristics and control accuracy of a novel proportional directional valve with independently controlled pilot stage," *ISA transactions*, vol. 93, pp. 218–230, 2019.

[6] Y. Li, R. Li, J. Yang, J. Xu, and X.Yu, "Recent advances in control strategies and algorithms for pilot-operated electro-hydraulic proportional directional valves," *Proc. IMechE. Part E: J. Process Mechanical Engineering*, early access.

[7] R. Carpenter, and R. Fales, "Mixed Sensitivity H-Infinity Control Design with Frequency Domain Uncertainty Modeling For a Pilot Operated Proportional Control Valve," *Proceedings of the ASME 2012 5th annual dynamic systems and control conference joint with the JSME 2012 11th motion and vibration conference*, Fort Lauderdale, 2012, pp. 17-19.

[8] Y. Li, R. Li, J. Yang, X. Yu, and J. Xu, "Review of recent advances in the drive method of hydraulic control valve," *Processes*, vol. 11, no. 9: 2537, 2023.

[9] Q. Zhong, E. Xu, T. Jia, H. Yang, B. Zhang, Y. Li, "Dynamic performance and control accuracy of a novel proportional valve with a switching technology-controlled pilot stage," *J. Zhejiang Univ. Sci. A*, vol. 23, no. 4, pp. 272-285, 2022.

[10] B. Jin, Y. Zhu, and W. Li, "Pid parameters tuning of proportional directional valve based on multiple orthogonal experiments method: method and experiments," *Applied Mechanics & Materials*, vol. 323, pp. 1166-1169, 2013.

[11] H. Wang, X. Wang, J. Huang, and L. Quan, "Performance improvement of a two-stage proportional valve with internal hydraulic position feedback," *Journal of Dynamic Systems Measurement and Contro*l, vol. 143, no. 7: 071005, 2021.

[12] B. Xu, Q. Su, J. Zhang, and Z. Lu, "Analysis and compensation for the cascade dead-zones in the proportional control valve," *ISA Transactions*, vol. 66, pp. 393-403, 2016.

[13] Z. Lu, J. Zhang, B. Xu, D. Wang, Q. Su, J. Qian, G. Yang, and M. Pan, "Deadzone compensation control based on detection of micro flow rate in pilot stage of proportional directional valve," *ISA Trans*, vol. 94, pp. 234-245, 2019.

[14] C. Wang, L. Quan, S. Zhang, H. Meng, and Y. Lan, "Reduced-order model based active disturbance rejection control of hydraulic servo system with singular value perturbation theory," *ISA Transactions*, vol. 67, pp. 455-465, 2017.

[15] X. Ji, Y. Wang, H. Xie, and C. Wang, "Nonlinear robust control of pump controlled single-rod actuator with observing and compensating modeling uncertainties," *ISA Transactions*, vol. 168, pp. 160-173, 2026.

[16] W. Shen and J. Wang, "An integral terminal sliding mode control scheme for speed control system using a double-variable hydraulic transformer," *ISA Trans*., vol. 124, pp. 386–394, 2019.

[17] X. Ji, C. Wang, Z Zhang, C. Shuai, and X Guo "Nonlinear adaptive position control of hydraulic servo system based on sliding mode back-stepping design method," *Proc. IMechE. Part I: J Systems and Control Engineering*, vol. 235, no. 4, pp. 474-485, 2021.

[18] B. Helian, Z. Chen, and B. Yao, "Constrained Motion Control of an Electro- Hydraulic Actuator Under Multiple Time-Varying Constraints," *IEEE Trans. Ind. Informatics*, vol. 19, no. 12, pp. 11878-11888, 2023.

[19] X. Ji, H. Xie, and C. Wang, "Research on characteristics and main stage spool displacement control method of multi-way valve controlled by proportional solenoid valve,". *Journal of Mechanical Engineering*, to be published.

[20] C. Krimpmann, G. Schoppel, I. Glowatzky, and T. Bertram, "Lyapunov-based self-tuning of sliding surfaces — methodology and application to hydraulic valves," *IEEE international conference on advanced intelligent mechatronics*, pp. 457-462, 2016.